Experimental Investigation of Lithium-Ion Cells Ageing under Isothermal Conditions for Optimal Lifetime Performance

Dr S. Landini[*,1], Prof. Tadhg S. O'Donovan[1]

[1]Institute of Mechanical, Process and Energy Engineering, School of Engineering and Physical Sciences, Heriot-Watt University, Edinburgh EH14 4AS, United Kingdom

Abstract

Lithium-Ion cell ageing is sensitive to cell temperature. Previous studies have investigated ageing under adiabatic or controlled environmental temperature (i.e., isoperibolic) conditions. Notably, these conditions do not impose a uniform cell surface temperature (i.e., isothermal condition) or a controlled cooling rate, as an active Thermal Management System (TMS) would. This leads to a clear interdependence between charge/discharge rates and cell temperature, due to the uncontrolled cell temperature history. Consequently, the separate influence of these variables on the cell performance cannot be investigated. In this study, the ageing of a 300mAh Lithium Cobalt Oxide (LCO Li-Ion) pouch cell under isoperibolic and isothermal conditions in the range of 0°C - 40°C is investigated. Each cycle comprises a CC-CV (constant current-constant voltage) charge of 1C and a CC discharge of 2C. Similar average ageing rates for isoperibolic and for isothermal conditions but at different reference temperatures were found. For example, an isoperibolic temperature condition of 25°C yielded a similar degrading rate as an isothermal condition at 30°C. This is mainly due to the effect of the cell self-heating (Joule heating) which increases the median operating temperature above that of the surroundings. These findings emphasise that uncontrolled cell thermal conditions lead to overall performance strongly dissimilar and randomly dependent on the transient heat transfer coefficient of isoperibolic TMS. Finally, an optimal isothermal condition that maximises the cell electrochemical efficiency and minimises its ageing is identified in the range of 25°C-35°C.

Keywords: Li-Ion cells; thermal management; isothermalisation; ageing effect; life performance

* Corresponding Author:
s.landini@hw.ac.uk (S. Landini)

Contents

Nomenclature

E	Electrical Energy	t	Time
HR	Heat Ratio	Δt	Time Period
P	Power	T	Temperature
Q	Heat	ΔT	Temperature Uniformity
$\dot{Q}$	Heating Rate	V	Voltage
r	Rate	η	Efficiency
SOH	State Of Health		

Subscripts

a	Ageing	ch	Chemical
act	Activation	opt	Optimum
all	All	set	Set
av	Average		

Glossary

CR	Charge Rate	LDPE	Low-Density Polyethylene
DR	Discharge Rate	OCV	Open Circuit Voltage
EOL	End of Life	PCM	Phase Change Material
DAQ	Data Acquisition	PGS	Pyrolytic Graphite Sheets
DOD	Depth of Discharge	PHS	Pump Hydro Storage
EESS	Electrical Energy Storage System	SMU	Source Measure Unit
EG	Expanded Graphite	TCE	Thermal Conductivity Enhancement
EV	Electric Vehicle	TMS	Thermal Management System

1 Introduction

Li-Ion cells have become essential components of many energy systems, from stationary to automotive applications [1–3]. They are characterised by high energy and power densities, therefore low volume and weight, compared to other chemistries [4]. However, Li-Ion cells operating life and economic competitiveness is still limited compared to other electrical energy storage systems (e.g. Pumped Hydro Storage) by the so-called ageing effect [5]. The ageing effect is characterised by the decrease in discharge capacity and energy of a Li-Ion cell with the number of charge/discharge cycles [6]. This is typically measured by the State Of Health (SOH), which is defined as the ratio of the actual energy discharged by a cell compared to its nominal value (i.e. a fresh un-aged cell). A condition of SOH lower than 80% signals the End-Of-Life (EOL) of a Li-Ion cell [1]. The ageing rate, r_a is typically used as indicator of the ageing of a Li-Ion cells throughout its operating life.

Importantly, previous literature shows that r_a is mainly dependent on temperature (Table 1), discharge rate (Table 2), charge rate, charge protocols, and state of charge range (Table 3) [1,4,5,7,8]. Waldmann et al. [4] analysed the ageing of cylindrical cells cycled at thermal chamber temperatures from -20°C to 70 °C, at CR=0.5C and DR=1C, and within a potential range of 2-4.2 V. A thermal chamber temperature of 25°C was shown to minimise the ageing effect. Also, the degradation was faster at low temperatures, due to lithium plating as the main ageing mechanism. At higher temperatures degradation was associated with Solid Electrolyte Interphase (SEI) growth. Similarly, Ramadass et al. [9] investigated the ageing of a 1.8Ah cylindrical cell under controlled lab temperatures. The cell was charged and discharged at CR=DR=0.56C. The minimal ageing rate was shown to occur at the lowest temperature tested equal to the lab temperature of 20°C. Dubarry et al. [10] tested prismatic and cylindrical 10Ah LiFePO4 cells of geometries at isoperibolic temperatures of 25°C and 60°C at CR=C/10 and DR=C/2. For both geometries, 25°C achieved the longest operating life. Similarly, Leng et al. [11] investigated the ageing rate of a 1.35Ah prismatic cell at CR=0.5C and DR=1C. Four different isoperibolic conditions were imposed (25°C, 35°C, 45°C, and 55°C) and 25°C resulted in the lowest ageing rate. Wu et al. [12] cycled 5Ah pouch cells at CR and DR of 1C at 10°C, 25°C, and 40°C. Uniquely in the literature, they indicated the difference between the isoperibolic temperature and the median cell surface temperature, the latter being 10.1°C, 27.5°C, and 41.5°C respectively. This difference was limited due to the low DR. From their results, an isoperibolic temperature of 40°C led to the fastest ageing.

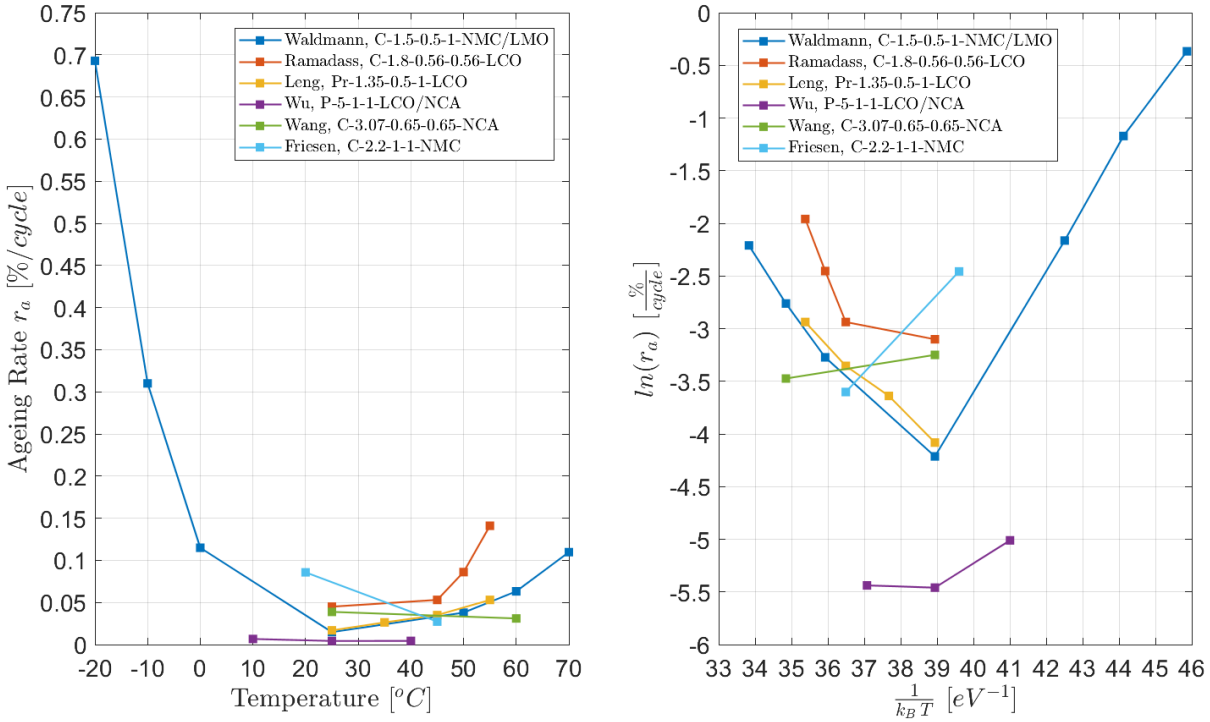

Figure 1: Ageing rate, r_a: effect of surrounding temperature (isoperibolic boundary condition). On the left, $r_a$as a function of surrounding temperature. On the right, Arrhenius plot, i.e. ln(r_a) as a function of Arrhenius term $\frac{1}{k_B T}$: the slope of the curve is equal to the equivalent activation energy E_{act} of the ageing mechanism. The legend code is: Author, x-y-z-j-k where x=geometry, y=capacity, z=CR, j=DR, k=chemistry.

In opposition to these studies, Wang et al. [13] reported a higher ageing effect at 25°C compared to 60°C for a 3.07Ah cylindrical cell cycled at CR=DR=0.65C. Similarly, Friesen et al. [14] tested 2.2Ah cylindrical cells with CR=DR=1C under two thermal chamber temperatures, 20°C and 45°C, where the latter guaranteed a lower degradation rate. Overall, there is evidence (Table 1, Figure 1) that the best ambient or surrounding temperature (different from cell temperature) to minimise a Li-Ion cell's ageing is greater or equal to 25°C.

Table 1: Ageing rate effect of surrounding temperature (isoperibolic boundary condition. Details on Li-Ion cell geometry, capacity, CR, DR and cathode chemistry.

Ref	Type	Cap	CR	DR	Chemistry	Temperature	Ageing Rate	T_{opt}
[4]	C	1.5	0.5	1	NMC-LMO	[-20,-10, 0, 25, 50, 60, 70]	0.01 - 0.69	25
[9]	C	1.8	0.56	0.56	LCO	[RT, 45, 50, 55]	0.034 - 0.141	25
[11]	Pr	1.35	0.5	1	LCO	[25, 35, 45, 55]	0.017 - 0.053	25
[12]	P	5	1	1	LCO-NCA	[10, 25, 40]	0.004 - 0.007	25
[13]	C	3.07	0.65	0.65	NCA	[25, 60]	0.031 - 0.039	60
[14]	C	2.2	1	1	NMC	[20, 45]	0.027 - 0.086	45

Legend: Cap=Capacity [Ah], C=Cylindrical, P=Pouch, Pr=Prismatic LCO=LiCoO2, LFP=LiFePO4, LMO=LiyMn2O4, NMC=LixNiyMnzCowO2 NCA=LixNiyCozAlwO2, T = Thermal Chamber Temperature [°C],
T_{opt}= Optimal Thermal Chamber Temperature [°C], r_a= Ageing Rate Min-Max [%]

Other studies investigated the effect of CR, DR, and cycling methodology on the ageing rate of Li-Ion cells, as reported in Table 2 and Table 3 respectively.

Table 2: Ageing Effect. Sensitivity to the DR

Ref	T	Type	Code	Cap	Cathode	CR	DR	r_a
[15]	25	C	-	1.9	NMC-LMO	0.5	0.04	0.0680
							0.20	0.0570
							0.50	0.0530
							1.00	0.0480
							2.00	0.0430
							5.00	0.1616
[16]	25	P	-	10.0	LTO	1.0	5.0	0.0036
							10.0	0.0020
[17]	25	C	-	1.4	LCO	0.7	1	0.0317
							2	0.0440
							3	0.0563
[18]	25	P	LCO1	3.3	LCO	1.0	1.0	0.0050
							25.0	0.0500
			LCO2	2.0	LCO		1.0	0.0060
							10.0	0.0429
			LCO3	3.0	LCO		1.0	0.1500
							10.0	0.3000
			LCO4	3.0	LCO		1.0	0.0117
							25.0	0.0750
			LCO5	3.0	LCO		1.0	0.0083
							25.0	0.0387
							45.0	0.0556
			LCO6	3.0	LCO		1.0	0.0387
							10.0	0.0857
			LCO7	2.4	LCO		1.0	0.0040
							25.0	0.0125
							45.0	0.0333
			LFP1	3.0	LFP		1.0	0.0083
							10.0	0.0632
			LFP2	2.5	LFP		1.0	0.0033
							10.0	0.0300
[19]	25	P	-	14.6	LMO	2.0	1.0	0.0032
							3.0	0.0038
							5.0	0.0042

Legend: Cap=Capacity [Ah], C=Cylindrical, P=Pouch, T = Thermal Chamber Temperature [°C], r_a= Ageing Rate [%/cycle], LCO=Lithium Cobalt Oxide, LTO=Lithium Titanate Oxide LMO=Lithium Manganese Oxide, LFP=Lithium Iron Phosphate NMC=Lithium Nickel Manganese Cobalt Oxide

Most evidence shows that higher CRs and DRs lead to faster ageing due to faster SEI growth and decomposition, electrodes cracking and/or exfoliation, and consequent loss of electrical contact. Also, adopting a CC instead of a CCCV charge methodology and imposing a resting period up to 2 days after 50 or 100 consecutive cycles can help to relax the Li-Ion cell, recover part of the lost energy capacity, increase the SOH, and decrease the overall ageing rate.

Table 3: Ageing Effect: Sensitivity to the CR and cycling mode.

Ref	T	Type	Cap	Cathode	CR	DR	Mode	r_a
[20]	34	Pr	25	NMC	1 2 3 4	1	CCCV	0.0075 0.0060 0.0150 0.1000
[21]	10	Pr	25	NMC	1	2	CCCV No rest CCCV Rest every 100 cycles	0.0278 0.0176
					2	1	CCCV No rest CCCV Rest every 100 cycles CCCV Rest every 50 cycles	0.0606 0.0541 0.0357
[22]	25	P	7	LFP	1	5	CCCV No Rest CC No Rest	0.0084 0.0054
[23]	25	C	1.5	NMC-LMO	0.5	1.0	CCCV No Rest CC No Rest	0.0200 0.0178

Legend: Cap=Capacity [Ah], C=Cylindrical, P=Pouch, Pr=Prismatic, T = Thermal Chamber Temperature [°C], r_a= Ageing Rate [%], LMO=Lithium Manganese Oxide, LFP=Lithium Iron Phosphate NMC=Lithium Nickel Manganese Cobalt Oxide

Importantly, however, the temperature controlled in these studies was the surrounding temperature of the cell, e.g. by using a thermal chamber or calorimeter chamber temperature (i.e. isoperibolic boundary condition), and not the cell's surface temperature (i.e. isothermal boundary condition). These two temperatures noticeably differ as discussed in Landini et al. [24], especially at high charge and discharge rates, a phenomenon called self-heating. As it is, the Li-Ion cell surface temperature was not controlled, and the effect of the rate of charge and discharge was never truly separated from the effect of the cell operating temperature both on average and as it varied over the cycle. In addition, previous literature mostly investigated the effect of temperature on Li-Ion cells' ageing effect at low CR/DR (maximum 1C) for cylindrical geometries. So, further research is needed on this matter for prismatic/pouch cells tested at broad temperature ranges (with an additional focus on temperature within the range of 10°C-50°C) and high CR/DR.

Therefore, the aim of this study is to apply the novel experimental approach proposed in Landini et al. [24]and evaluate the effect of different isothermal conditions (i.e. imposing a constant and uniform Li-Ion cell surface temperature) on the ageing effect of a Li-Ion pouch cell. This approach truly imposes an isothermal condition compared to the isoperibolic boundary condition used in previous studies [4,9,11,12,13,14]. In this way, the dependence of the cell temperature history to charge/discharge rates due to the cell self-heating effect by Joule ohmic losses, typically non negligible for high rates, is depleted and the results can be truly used to analyse the only effect of temperature on the ageing mechanisms.

2 Methodology

The test rig components, configuration, and cells' cycling methodology used in this study are extensively reported in Landini et al. [24]. The properties of the Li-Ion pouch cells and the overall test rig uncertainty for each quantity of interest are reported in Table 4 for reference. The AKKU300 Li-Ion polymers pouch cells used in this study were characterised by a nominal voltage of 3.7 V, a capacity of 300 mAh, dimensions 32 mm × 23 mm × 4.8 mm, a mass of 7.02 gr, and a specific heat capacity of 1479 J/kg K. It should be noted that the specific heat capacity uncertainty of 13.9% reported in Table 4 is relatively high when compared with previous literature. However, due to the isothermalisation capability of the test rig and the consequent negligible cell temperature variation throughout the ageing tests, the enthalpy variation component of the cell heat generation rate is trivial, therefore the potential impact of the specific heat capacity uncertainty on the evaluation of the cell heat generation rate is negligible.

Identical cells (same model, manufacturer, provider, batch), have been firstly conditioned (i.e. cycled 5 times at CR=DR=1C at 25°C) to activate properly the cathode chemistry, as reported in previous literature, and verify the property agreement among all cells [4]. The discharged capacity and energy typically increased throughout the consecutive five conditioning cycles as the electrodes (mostly the cathode) capacity was enhanced by creating new additional de-intercalation spots by thermal expansion and contraction mostly triggered at the discharge phase.

Table 4: Li-Ion cells properties and test rig uncertainty [24]

Property	**Li-Ion Cell**
Name	AKKU300
Technology	Li-Ion Polymers
Voltage [V]	3.7
Capacity [mAh]	300
Length [mm]	32
Width [mm]	22
Height [mm]	4.8
Mass [g]	7.02
Density [kg/m^3]	2077
Specific Heat Capacity [J/kg K]	1479

Quantity	**Symbol**	**Uncertainty**
Temperature	T	0.19°C
Temperature Average	T_{av}	0.09°C
Temperature Uniformity	ΔT	0.27°C
Specific Heat Capacity	c_p	13.9%
Voltage	V	0.07%

Current	I	0.13%
Electrical Power	P	0.15%
Heat Generation Rate	$\dot{Q}$	8.12%
Efficiency	η	0.83%
Heat Ratio	HR	8.12%

Each cell has been cycled continuously at a set controlled isothermal condition (i.e. stable average surface cell temperature). This boundary condition has been imposed by using the novel test rig and methodology described in a previous study by Landini and O'Donovan [24]. The novel test rig emulates an active Li-Ion cell thermal management and it is composed of a thermal chamber, a micro wind tunnel, and a control system. The cell surface is exposed to a thermal boundary condition where the convective heat transfer coefficient is kept constant and, by tuning the wind temperature to control the temperature difference between cell and wind, a controlled and dynamic surface heat flux balances the highly variable cell heat generation rate. This ensures a constant cell surface temperature both temporally and spatially. However, it must be pointed out that the median Biot number in respect to the heat transfer along the transversal direction (i.e. thickness) of the pouch cell was around 0.31, suggesting a good uniformity of the cell body temperature. Crucially, this is different from a standard uniform environmental condition (defined as isoperibolic) where the cell surface temperature and critically the rate of heat transfer from the cell would be different from an active TMS. For more details, the reader is referred to Landini and O'Donovan [24].

Each ageing test was composed of consecutive charge and discharge cycles under CR=1C and DR=2C until its End Of Life (EOL), defined as the condition of a SOH (based on the discharged energy) lower or equal than 80%. The DR of 2C has been selected to maximise the ageing rate (i.e. minimise the EOL and the ageing period), to test as many temperatures as possible, while guaranteeing consistent isothermal conditions, i.e. lowering the temperature uniformity ΔT on the Li-Ion pouch cell surface. In this regard, it must be highlighted that the methodology and test rig used in this study and reported in Landini et al. [24] maintains an ideal isothermal condition for DR up to 2C. Importantly, the heat transfer coefficient applied at the cell's surface, characterised by an average, median, and standard deviation of 130 $\frac{W}{m^2K}$, 128 $\frac{W}{m^2K}$ and 9.4 $\frac{W}{m^2K}$ respectively at set temperatures T_{set} in the range of 0°C-40°C, and the control methodology guarantee a cell average surface temperature T_{av} constant and equal to the set temperature T_{set} with an error lower than 0.2K and a temperature uniformity ΔT lower than 4°C. The lower the ΔT, the more the Li-Ion pouch cell thermal boundary condition approaches an ideal isothermal condition. The effect of the cell self-heating due to high DRs (i.e. high electrical currents and high heat generation rates) is limited by this approach which imposes an actual isothermal and not

only isoperibolic thermal boundary condition on the Li-Ion cell compared to previous literature. Therefore, a clearer distinction of the separate effect of temperature and DR is in this test rig possible.

3 Results

3.1 Effect of Isothermal Conditions on Ageing

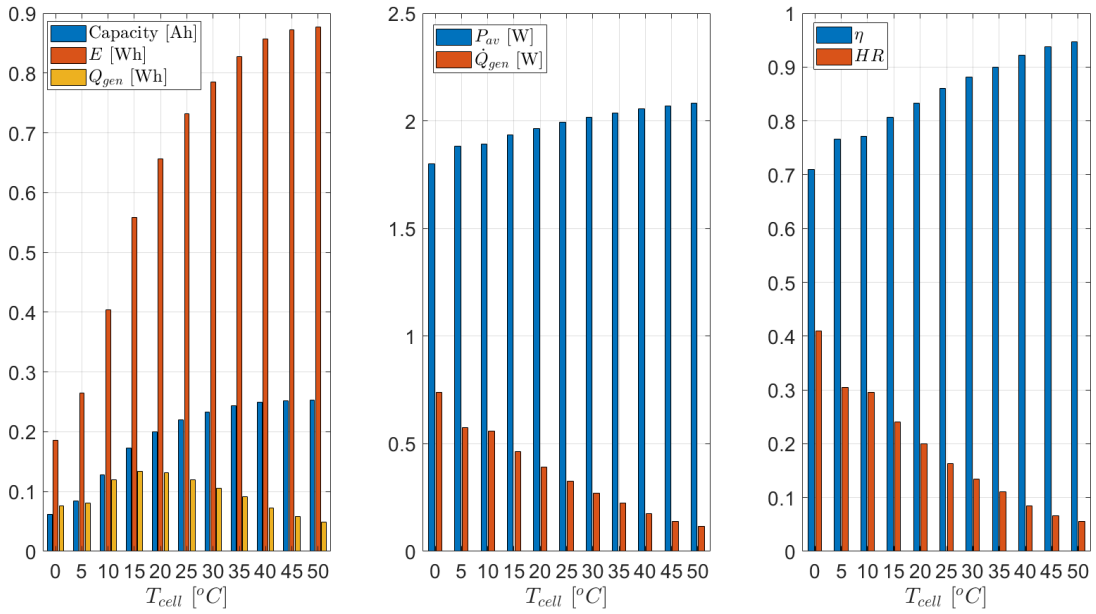

Figure 2: Electrical, thermal, and electrochemical discharge performance of Li-Ion pouch cells under DR=2C in un-aged conditions for different isothermal conditions. The results for temperatures equal to 0°C, 10°C, 20°C, 30°C, 35°C, and 40°C are taken from the cells tested for the ageing effect and whose ageing rates are reported in the following. The additional tests at 5°C, 15°C, 45°C, and 50°C were taken from different cells for each temperature value to give a broader insight.

The electrical, thermal, and electrochemical performance of the Li-Ion pouch cells employed for the ageing tests in the so-called fresh or initial condition (first cycle, no ageing effect) are reported in Figure 2 and Table 5 for CR=1C, DR=2C, and cell surface temperature in the range of 0°C-50°C. The results for temperatures equal to 0°C, 10°C, 20°C, 30°C, 35°C, and 40°C are taken from the first cycle of the cells tested for the ageing effect. The additional tests at 5°C, 15°C, 45°C, and 50°C were taken from a different cell for each temperature value and added to the graph to give broader insight. As previously highlighted in Landini et al. [24], at a fixed CR (in this study 1C) and DR (in this study 2C) Li-Ion cells deliver more electrical energy and dissipate less heat when cycled at higher cell temperatures, leading to higher electrochemical efficiencies. This would indicate that high temperatures should be employed to maximise the performance of a Li-Ion cell if the user is not concerned about the detrimental effect on the cell age that high temperatures trigger after a limited number of cycles. The

entire dataset collected within the Li-Ion cell ageing tests can be found in [25] divided for all the isothermal conditions imposed for the reader's reference.

Table 5: Electrical, thermal, and electrochemical discharge performance of Li-Ion pouch cells under DR=2C in un-aged conditions for different isothermal conditions. The results for temperatures equal to 0°C, 10°C, 20°C, 30°C, 35°C, and 40°C are taken from the cells tested for the ageing effect and whose ageing rates are reported in the following. The additional tests at 5°C, 15°C, 45°C, and 50°C were taken from different cells for each temperature value to give a broader insight.

T_{set}	Δt	DOD	Cap	E	P_{av}	Q	$\dot{Q}_{av}$	η	HR
0	371	20.6%	62	186	1.801	76	738	70.9%	41.0%
5	506	28.1%	84	265	1.884	81	574	76.7%	30.5%
10	768	42.6%	128	404	1.892	119	559	77.2%	29.6%
15	1040	57.7%	173	558	1.933	134	464	80.7%	24.0%
20	1203	66.8%	200	656	1.964	131	392	83.4%	20.0%
25	1321	73.3%	220	731	1.993	119	325	85.9%	16.3%
27.5	1362	75.7%	227	758	2.003	112	296	87.1%	14.8%
30	1402	77.8%	233	785	2.016	105	270	88.2%	13.4%
35	1462	81.1%	243	827	2.037	92	225	90.0%	11.1%
40	1501	83.3%	250	857	2.056	73	175	92.2%	8.5%
45	1516	84.1%	252	872	2.070	58	138	93.8%	6.7%
50	1517	84.2%	253	877	2.082	49	116	94.7%	5.6%

Legend: T_{set}= Set Temperature [°C], Δt = Test Period [s] DOD= final DOD, Cap = discharged capacity [mAh] E = discharged energy [mWh], P_{av}=average power [W], Q = heat generation [mWh], $\dot{Q}_{av}$ = average heat generation rate [mW], η =discharge efficiency, HR=Heat Ratio

Figure 3 and Table 6 show the SOH [%] (based on the discharged energy) variation with the number of cycles n (i.e. ageing process) and the related ageing rate r_a [%/cycle] at different isothermal conditions (i.e. different stable and uniform Li-Ion cell surface temperature T_{cell}) for Li-Ion cells cycled under CR=1C and DR=2C. The duration of each test, i.e. the End Of Life (EOL), is based on a condition of SOH=80% as used in literature and based on typical Li-Ion cells warranty agreements. Importantly, a single ageing rate r_a (to be taken as the average overall value throughout a Li-Ion cell operating life) is calculated by linear regression of the SOH vs number of cycles as shown in Figure 3.A and is equal to the regression line slope. This single value r_a can be exclusively reported, as proposed in previous literature [4]. However, this approach does not capture the potential variation of the ageing rate throughout the cell operating life due to different ageing mechanisms.

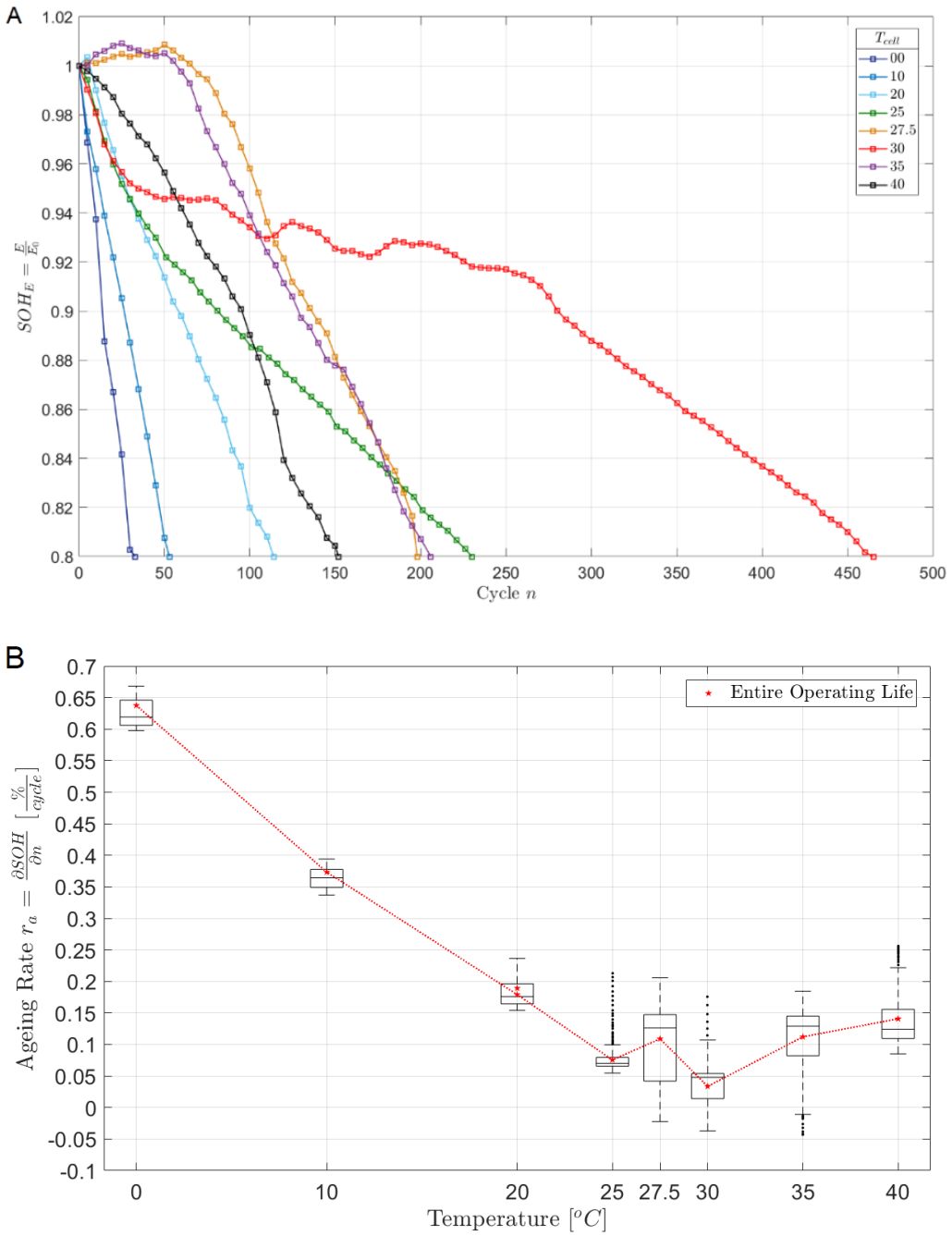

Figure 3: Ageing of a Li-Ion cell at different isothermal conditions under CR=1C and DR=2C: SOH variation with number of cycles n (A) and ageing rate r_a (B). The ageing rate r_a (B) is calculated by linear regression of the SOH vs number of cycles n and is equal to the regression line slope. A single r_a value can be reported by applying a single regression through the entire operating life of the cell (red line in B, as proposed in previous literature [83]) or a forward $r_a(n)$ can be calculated for each cycle n of the operating life adopting a forward-moving linear regression of period 25 cycles (arbitrarily selected as statistically meaningful for the regression procedure and small enough to capture the ageing rate variation) and a box-plot (black in B) is then used to emphasise the $r_a(n)$ variation.

Therefore, a novel forward $r_a(n)$ is proposed and calculated for each cycle n adopting a forward-moving linear regression of period 25 cycles (arbitrarily selected as statistically meaningful for the regression procedure and small enough to capture the ageing rate variation). In addition, statistics such as the $r_a(n)$ quantiles ($r_a(n)^{q\%}$) and standard deviation ($r_a(n)^{sd}$), reported in Table 6 and exemplified within the box plots in Figure 3.B, are used to emphasise the $r_a(n)$ variation.

The results show how the ageing process is highly sensitive to the Li-Ion cell temperature. Both high and low temperatures lead to strong ageing and consequently short operating life (i.e. quick EOL). The temperature which minimises the ageing and guarantees the longest operating life appears to be 30°C (EOL=450 cycle, r_a=0.034 %/cycle), while temperatures lower than 20°C lead to a r_a of more than tenfold. In addition, higher temperatures of 35°C and 40°C lead to an increase of the r_a around 3 to 4 times respectively by comparison with 30°C.

Table 6: Ageing of a Li-Ion cell at different isothermal conditions under CR=1C and DR=2C: SOH variation with number of cycles n (A) and ageing rate r_a (B). The ageing rate r_a (B) is calculated by linear regression of the SOH vs number of cycles n and is equal to the regression line slope. A single r_a value can be reported by applying a singular regression through the entire operating life of the cell (red line in B, as proposed in previous literature [83]) or a forward $r_a(n)$ can be calculated for each cycle n of the operating life adopting a forward-moving linear regression of period 25 cycles (arbitrarily selected as statistically meaningful for the regression procedure and small enough to capture the ageing rate variation) and a box-plot (black in B) is then used to emphasise the $r_a(n)$ variation. In bold, the optimal thermal boundary condition.

T_{cell}	r_a	$r_a(n)^{q1\%}$	$r_a(n)^{q25\%}$	$r_a(n)^{q50\%}$	$r_a(n)^{q75\%}$	$r_a(n)^{q99\%}$	$(r_a(n)^{sd}$
0	0.638	0.598	0.606	0.619	0.646	0.668	0.026
10	0.373	0.337	0.349	0.364	0.378	0.394	0.017
20	0.179	0.155	0.164	0.176	0.196	0.236	0.022
25	0.076	0.056	0.066	0.070	0.079	0.204	0.029
27.5	0.109	-0.022	0.042	0.126	0.147	0.205	0.069
30	**0.034**	**-0.036**	**0.014**	**0.048**	**0.054**	**0.126**	**0.030**
35	0.112	-0.040	0.082	0.129	0.145	0.183	0.058
40	0.141	0.086	0.109	0.124	0.156	0.255	0.049

Legend: T_{cell}=Cell Temperature [°C], r_a=ageing rate [%/cycle]

It is also interesting to note how the shape of the SOH curve shown in Figure 3 change for each ageing test conducted and it has no clear dependence on the temperature itself. For instance, cells tested at T_{cell} of 0°C, 10°C, 20°C, and 40°C show a quasi-consistent decrease of the SOH without an appreciable change in the r_a (i.e. slope of SOH in Figure 3.A). This is reflected by the contained variation of the $r_a(n)$ shown in Table 6 and in the extension of the boxplots and absence of outliers in Figure 3.B. Also, tests conducted at 27.5°C and 35°C

showed an apparent gain in discharge energy (i.e. negative $r_a(n)$ shown in the lower extents of the boxplots in Figure 3.B and in the $r_a(n)^{q1\%}$ in Table 6) in the first 50 cycles of the ageing process. This behaviour, similarly, to the conditioning tests previously mentioned, are possibly due to the creation of additional intercalation de-intercalation spots within the cell electrodes which were potentially triggered by the temperatures at which the cells were exposed. Finally, cells tested at 25°C and 30°C showed a first sharp decrease of the SOH (i.e. high $r_a(n)$) up to 50 cycles; this is clearly shown by the presence of high-value outliers within the boxplots of Figure 3.B, especially for 25°C. After this period, the ageing rate decreased for both temperatures; however, 30°C experienced a quasi-plateau phase (Figure 3.B, from cycle 50 to 250) where an alternate local gain of SOH has been captured by the negative value of $r_a(n)$ shown within the lower extents of the boxplot in Figure 3.B and Table 6.

Overall, it could be inferred that low temperatures (i.e. lower than or equal to 20°C) are more inclined to lead to an ageing effect characterised by a quasi-constant $r_a(n)$, i.e. ageing caused by a consistent mechanism that has been identified in previous literature [1,4] to be lithium plating and dendrite formation. This mechanism leads to a typical loss of lithium inventory and active anode material, causing the loss of capacity, energy, and power [1,8].

On the other hand, high temperatures seem to lead to a more inconsistent ageing process where the $r_a(n)$ varies along the cell operating life. This behaviour typically results in a change in the ageing rate (i.e. an increase or decrease of the $r_a(n)$), leading in some cases to apparent ageing plateaus or even energy gains (i.e. SOH recovery). As mentioned in previous studies [1,4], these appreciable variations of the $r_a(n)$ could be related to either a change of the ageing mechanism or a combination of several ageing mechanisms that are triggered in synchronous. The mechanisms involved in this temperature range are typically SEI growth and SEI, electrolyte, and binder (connection between electrodes and current collectors) decomposition [1,8].

Also, it should be noted that different batches were used and this may have had an influence on the behaviour of the SOH. Precisely, three different batches were employed: batch 1 (tests 20°C, 25°C, 40°C), batch 2 (tests 27.5°C, 35°C), and batch 3 (tests 10°C, 30°C). Specifically, the unusual behaviour highlighted for tests conducted at 27.5°C and 35°C could have been influenced by the fact that a different batch was employed. This is interesting additional information as it would suggest that cells characterised by the same geometry, chemistry, model, manufacturer, and provider can potentially express a different ageing process simply due to the manufacturing process they have been through and not necessarily to the isothermal condition imposed

under operational cycling. This is considered to be more probable when low-cost commercial cells (like the model used in this experimental campaign) are employed as the less stringent manufacturing protocols lead to Li-Ion cells specifics inconsistency among different batches and units.

3.1.1 Repeatability test

Ageing tests have been conducted twice by imposing an ideal isothermal boundary condition of 20°C on two cells, where the first cell is the same reported in the previous section. The results of the SOH and ageing rate, both overall average r_a and $r_a(n)$ (computed by forward moving linear regression of period 25 cycles) are reported in Figure 4 and Table 7.

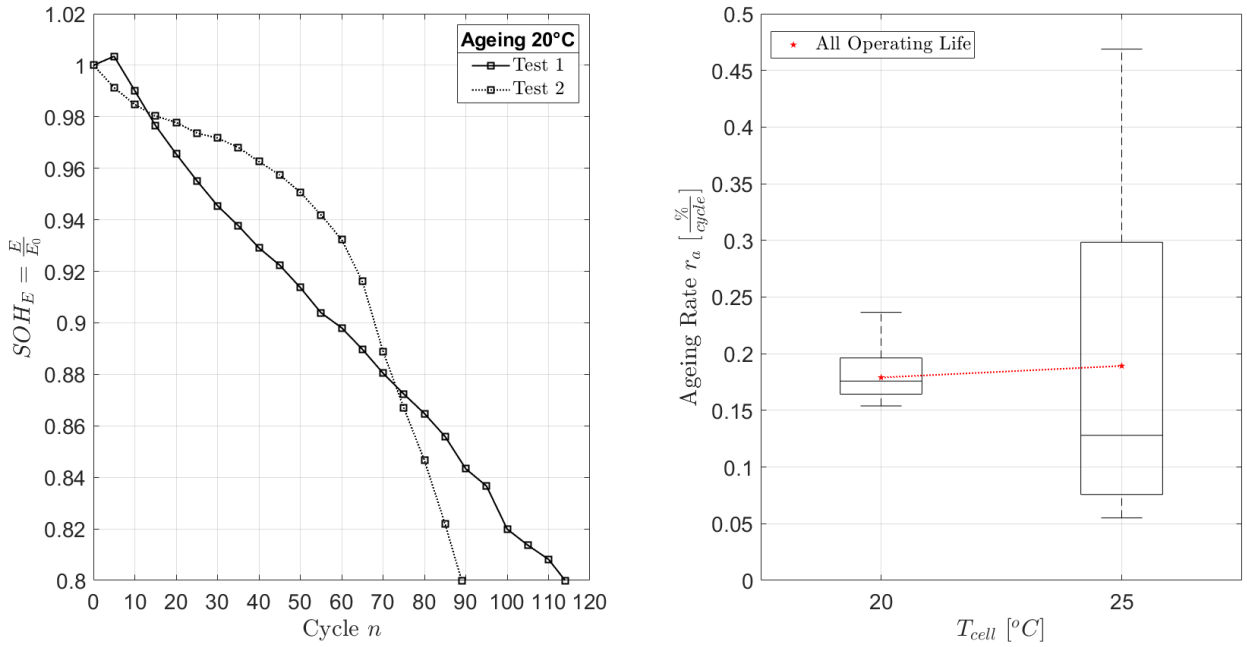

Figure 4: Repeatability tests for ageing effect under an isothermal condition of 20°C. On the left (A), the variation of SOH with the number of cycle n. On the right (B), a single value r_a can be reported by applying a singular regression through the entire operating life of the cell (in red) or a forward-moving $r_a(n)$ can be calculated for each cycle n of the operating life adopting a forward-moving linear regression of period 25 cycles and a boxplot (in black) is reported to emphasise the $r_a(n)$ variation.

The two Li-Ion cells (Test 1, Test 2) are cycled under the same electrical regime (CR=1C, DR=2C) and with the same isothermal boundary condition, but as shown have different SOH variation. Figure 4 shows that the cell of Test 1 aged consistently, with an ageing rate that varies minimally throughout the operating life (as shown by the statistics of the forward-moving $r_a(n)$ in Table 7). However, when the test is repeated (Test 2), the cell experiences a different SOH path, with a lower ageing rate at the beginning (as shown by the lower extents of the forward-moving $r_a(n)$ box-plot in Figure 4 and the $r_a(n)^{q1\%}$ in Table 7), an ageing acceleration after the 30th

cycle, a similar $r_a(n)$ compared to Test 1 in between cycles 40 and 60 (as shown by the similar $r_a(n)^{q50\%}$ in Table 7), and followed by significant ageing acceleration until reaching its EOL (as shown by the higher whisker of the $r_a(n)$ box-plot in Figure 4 and the $r_a(n)^{q99\%}$ in Table 5.3).

Overall, it can be stated that the ageing process of cells under the same electrical regime and thermal boundary condition can lead to a similar overall ageing rate (with a relative variation of around 6% as shown in Table 7) but with an appreciably different ageing path, which can be either consistent or variable (i.e. characterised by SOH plateaus and ageing acceleration). It must be finally mentioned that previous literature, like the one mentioned in the following section, typically reports a single value of ageing rate (i.e. the single r_a above mentioned) or report the ageing data for broad cycle steps, and therefor not reporting the potential local ageing variation.

Table 7: Repeatability tests for ageing effect under the isothermal condition of 20°C. On the left (A), the variation of SOH with number of cycle n. On the right (B), a single value r_a can be reported by applying a singular regression through the entire operating life of the cell (in red) or a forward-moving $r_a(n)$ can be calculated for each cycle n of the operating life adopting a forward-moving linear regression of period 25 cycles and a boxplot (in black) is reported to emphasise the $r_a(n)$ variation.

Test	$\boldsymbol{r_a}$	$\boldsymbol{r_a(n)^{q1\%}}$	$\boldsymbol{r_a(n)^{q25\%}}$	$\boldsymbol{r_a(n)^{q50\%}}$	$\boldsymbol{r_a(n)^{q75\%}}$	$\boldsymbol{r_a(n)^{q99\%}}$	$\boldsymbol{(r_a(n)^{sd}}$
1	0.179	0.155	0.164	0.176	0.196	0.236	0.022
2	0.189	0.055	0.076	0.128	0.298	0.468	0.139
Variation	6%	64%	54%	27%	52%	98%	531%

Legend: T_{cell}=Cell Temperature [°C], r_a=ageing rate [%/cycle]

3.1.2 Effect of thermal boundary condition

Three ageing tests have been conducted using the thermal chamber to impose a standard isoperibolic condition at 10°C, 25°C, and 35°C. These tests have been compared to the isothermal tests and reported in terms of SOH profiles in Figure 5. A consistent difference in conducting isoperibolic or isothermal tests is apparent from the results presented. Also, it is interesting to notice that an isoperibolic condition of 25°C leads to an overall average ageing rate close to an isothermal condition of 30°C, an isoperibolic condition of 10°C leads to an overall average ageing rate close to an isothermal condition of 20°C, while an isoperibolic condition of 35°C leads to an overall average ageing rate not dissimilar to an isothermal condition of 35°C. This is mainly the effect of the cell self-heating due to Joule effect which forces the cell to operate at a median temperature higher than the surroundings. Importantly, this emphasises again that the uncontrolled thermal condition of the cell

leads to overall cell performance strongly dissimilar and randomly dependent on the transient heat transfer coefficient of isoperibolic TMS.

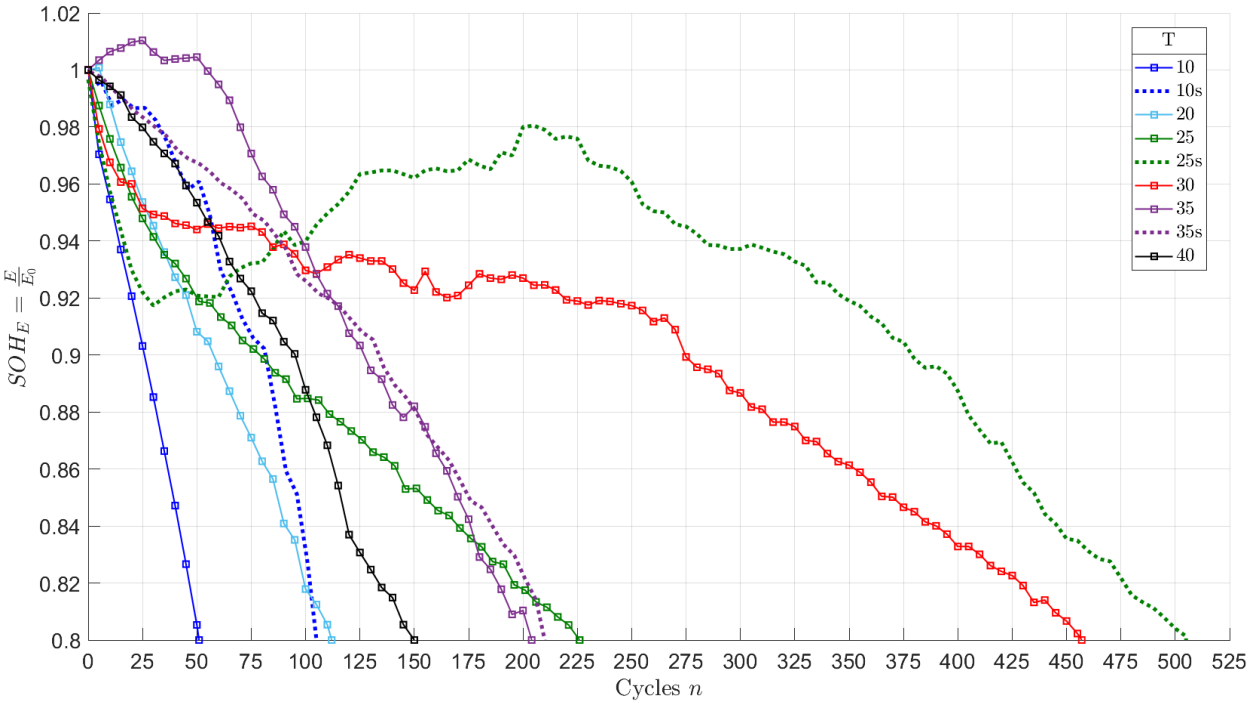

Figure 5: Ageing of a Li-Ion cell: effect of isothermal and isoperibolic (also termed static, labelled as "s") thermal boundary conditions under CR=1C and DR=2C. The graph shows the SOH variation with the number of cycles n.

3.1.3 Comparison with previous literature

The results of the experimental campaign have been compared with previous literature focused on the effect of temperature on the Li-Ion cell ageing effect, which has been critically reviewed in the introduction. It must be emphasised again that all these previous experimental studies controlled the surrounding temperature of the cell and not the cell surface temperature itself, i.e. an isoperibolic boundary condition was imposed and not a truly isothermal condition on the cell surface. This must be carefully considered for instance when looking at graphs plotting ageing data on a temperature axis where for the previous studies this axis represents the surrounding temperature and for the current study, it reflects the actual cell temperature.

Figure 6 and Table 8 report the comparison of the ageing rate r_a (i.e. the single average ageing rate mentioned in the previous section) for all studies reported in the literature and the current experimental campaign. Before drawing any conclusion by comparing the r_a found in these studies, it must be emphasised that all these studies,

including the current research, have been carried out testing different Li-Ion cells, specifically different geometries (cylindrical, pouch, prismatic), capacities (from 0.3 up to 5Ah), cathode chemistries (even if all lithium-based and sharing a graphite-based anode), CR (from 0.5C to 1C), and DR (from 0.5C to 2C).

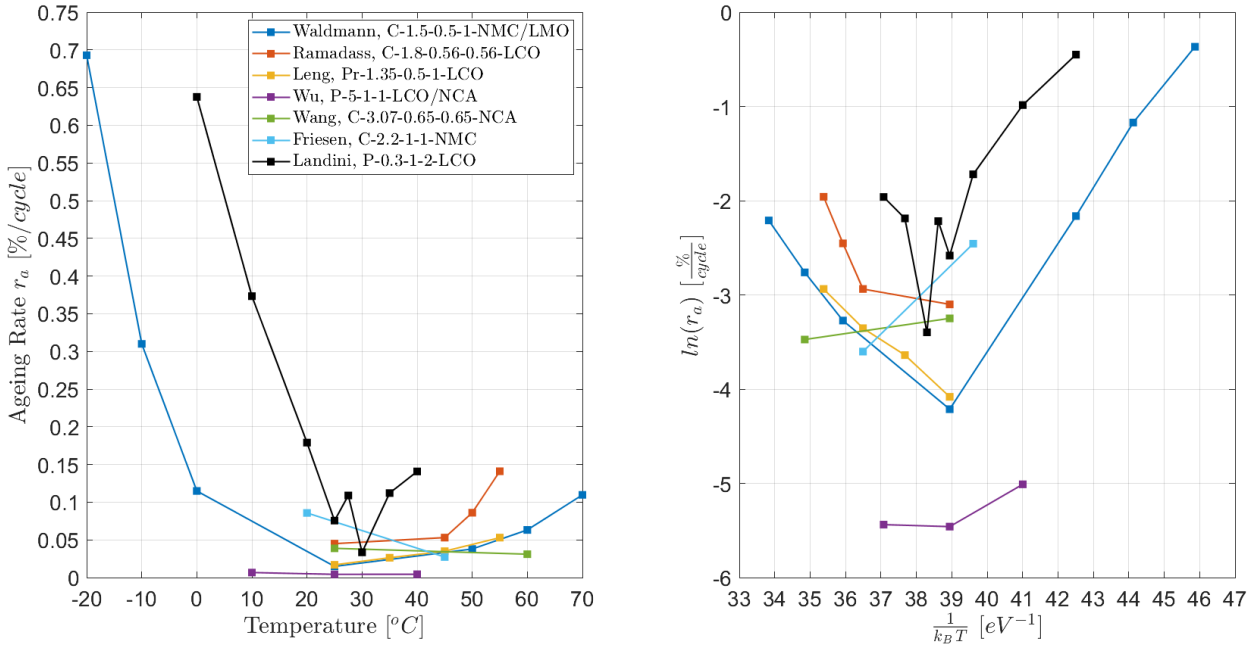

Figure 6: Ageing rate r_a sensitivity to Li-Ion cell thermal boundary condition: isoperibolic (surrounding temperature) for previous literature, isothermal (cell temperature) for the current study. On the left (A), r_a in function of temperature. On the right (B), Arrhenius plot, i.e. ln(r_a) in function of Arrhenius term $\frac{1}{k_B T}$: the slope of the curve is equal to the equivalent activation energy E_{act} of the ageing mechanism. The legend code is: Author, x-y-z-j-k where x=geometry, y=capacity, z=CR, j=DR, k=chemistry. Chemistry: LCO=LiCoO2, LFP=LiFePO4, LMO=LiyMn2O4, NMC=LixNiyMnzCowO2, NCA=LixNiyCozAlwO2.

Most importantly, the reviewed studies, based on an isoperibolic boundary condition, have been conducted at variable disuniform different cell temperatures. This would suggest therefore that even when experiments were carried out by different authors, using identical cells under similar cycle regimes and imposing the same isoperibolic boundary condition (i.e. the same thermal chamber or calorimeter temperature), different cell operating temperatures were experienced due to a different heat flux (or heat transfer coefficient) imposed on the Li-Ion cell surface. Importantly, the difference between the surrounding temperature and the cell surface temperature when imposing an isoperibolic boundary condition would be typically enhanced by high CR/DR and low temperatures (e.g. lower than 20°C), two conditions that lead to higher heat generation rates as extensively reported in the introduction section and Landini et al. [24]. However, there is still value in looking at these ageing tests together to draw interesting and valuable conclusions.

Table 8: Ageing rate r_a sensitivity to Li-Ion cell thermal boundary condition: isoperibolic (surrounding temperature) for previous literature, isothermal (cell temperature) for the current study. In bold, the optimal thermal boundary condition for each study.

Ref	Authors	Type	Cap	Cathode	CR	DR	T	r_a
[4]	Waldmann	C	1.5	NMC-LMO	0.5	1	-20	0.693
							-10	0.310
							0	0.115
							25	**0.015**
							50	0.038
							60	0.063
							70	0.110
[9]	Ramadass	C	1.8	LCO	0.56	0.56	**25**	**0.045**
							45	0.053
							50	0.086
							55	0.141
[11]	Leng	Pr	1.35	LCO	0.5	1	**25**	**0.017**
							35	0.026
							45	0.035
							55	0.053
[12]	Wu	P	5	LCO-NCA	1	1	10	0.007
							25	**0.004**
							40	0.005
[13]	Wang	C	3.07	NCA	0.65	0.65	25	0.039
							60	**0.031**
[14]	Friesen	C	2.2	NMC	1	1	20	0.086
							45	**0.027**
	This study	P	0.3	LCO	1	2	0	0.638
							10	0.373
							20	0.179
							25	0.076
							27.5	0.109
							30	**0.034**
							35	0.112
							40	0.141

Legend: Cap=Capacity [Ah], C=Cylindrical, P=Pouch, Pr=Prismatic r_a=ageing rate [%/cycle], T=temperature (surrounding or cell) [°C], LCO=$LiCoO_2$, LFP=$LiFePO_4$, LMO=$Li_yMn_2O_4$ NMC=$Li_xNi_yMn_zCo_wO_2$, NCA=$Li_xNi_yCo_zAl_wO_2$

Figure 6 (left) clearly shows that the current study found a similar sensitivity to the r_a to the temperature, where an optimal thermal condition is identified (30°C) and the ageing rate increases for both lower and higher values. It is also interesting that this optimal temperature is not far from the 25°C indicated by most of the previous studies (Waldmann et al. [4], Ramadass et al. [9], Leng et al. [11], Wu et al. [12]), considering that an isoperibolic temperature of 25°C would translate to a higher cell temperature (a difference less negligible for high CR and DR), approaching the 30°C indicated by this experimental campaign. It must be pointed out however that the

studies by Wang et al. [13] and Friesen et al. [14] indicated a reverse r_a trend with a lower ageing effect for increasing temperatures up to or above 45°C.

Table 9: Arrhenius (Figure 5.11 B) E_{act} of ageing mechanism. The ln(r_a) in function of an Arrhenius term 1 is plotted and the slope of each curve, equal to the equivalent activation energy E_{act} of the ageing process, can be used to identify a change in the ageing mechanism with a variation of the operating temperature.

Ref.	Authors	T_{opt}*	$E_{act}^{T>T_{opt}}$	$E_{act}^{T<T_{opt}}$
[4]	Waldmann et al.	25	-0.382	0.56
[9]	Ramadass et al.	25	-0.272	-
[11]	Leng et al.	25	-0.313	-
[13]	Wang	60	-	0.055
[14]	Friesen et al.	45	-	0.368
-	This study	30	-1.164	0.596

Legend: T_{opt}=optimal temperature [°C], T =surrounding or cell* temperature [°C], E_{act}=ageing mechanism activation energy [eV]

Also, the current experimental evidence shows a consistently higher ageing rate throughout the entire temperature range which could be due, in part, to the higher CR and DR imposed through the cell cycling, which theoretically would intensify the ageing mechanism related to high temperatures (SEI growth and decomposition) and trigger additional mechanisms such as graphite (i.e. anode) exfoliation, structural disordering, loss of electrical contact, and electrodes cracking.

Moreover, an Arrhenius plot (Figure 6 right) is used to report the same ageing rate results. By plotting the ln(r_a) as a function of an Arrhenius term 1, the slope of each curve, equal to the equivalent activation energy of the ageing process, can be used to identify a change in the ageing mechanism with a variation of the operating temperature. The current study shows a similar qualitative trend when compared to the previous experimental investigations (most evidently Waldmann et al. [4], being the only complete study to go below and above the identified optimal temperature), confirming a change of slope (i.e. ageing mechanism) for temperatures higher or lower the optimal value of 30°C. Interestingly, however, the trend seems to appreciably diverge from being purely linear (as noticed in Waldmann [4] and Leng [11] studies), a phenomenon previously experienced within the investigation of Ramadass et al. [9].

Even if the Arrhenius plot trend for each study is not exactly linear, the equivalent E_{oact} for temperatures higher or lower than the optimal value T_{opt} have been computed by linear regression on the curves of Figure 6 (right) and are reported in Table 9 for reference. It might be inferred that the activation energy of the ageing

mechanisms found in the current research at low temperatures (equal to 0.596 eV) is comparable to previous literature while the ageing mechanism at high temperatures (equal to -1.164 eV) is greater, at approximately 3 times higher than the median values found in the literature. This may give evidence to support the assertion that the higher CR and DR employed in this experimental campaign has intensified the ageing mechanism related to high temperatures (SEI growth and decomposition).

3.3 Overall life performance

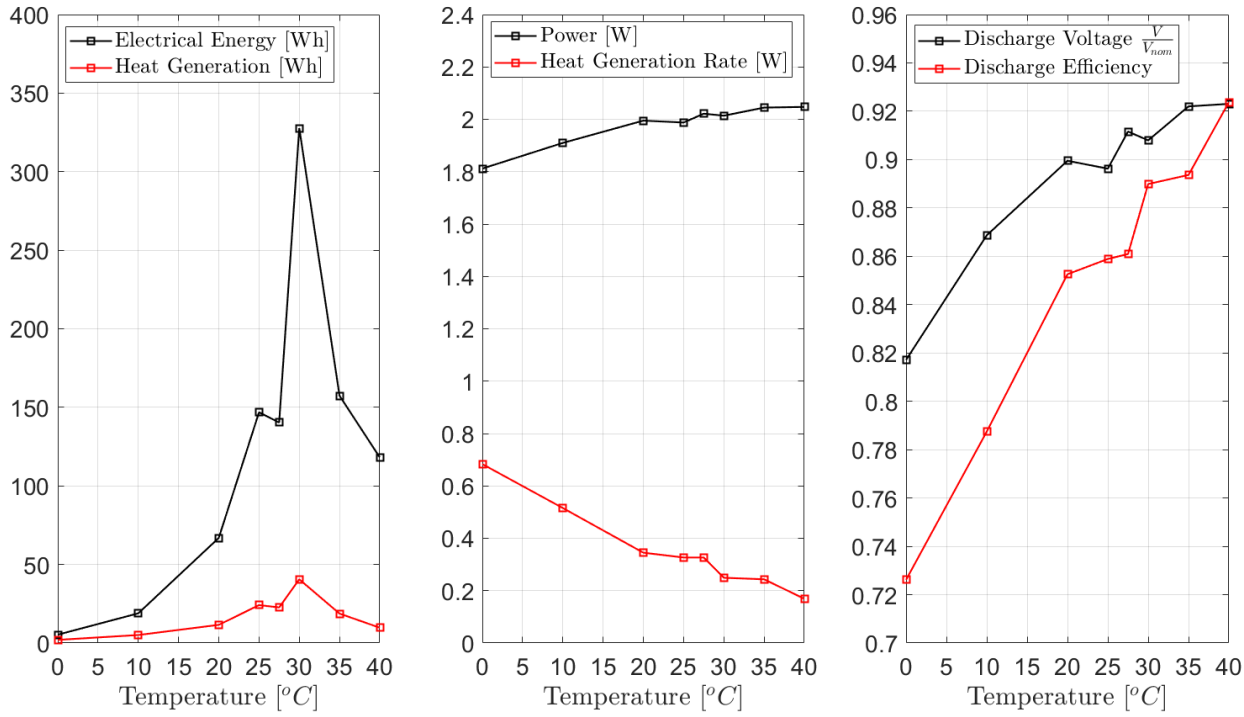

Figure 7: Overall operating life discharge performance of Li-Ion cells at different isothermal conditions. The average discharge voltage is reported relative to the nominal V_{nom} of the cell, as reported in the manufacturer specifics and equal to 3.7 V.

It is important to focus on the overall life performance of the Li-Ion cell tested at different isothermal conditions. Figure 7 and Table 10 report the overall operating life performance (sum of all the cycles of the ageing tests, i.e. from the first cycle until the EOL) in terms of life discharged capacity and electrical energy, life average operating voltage V_{av} (calculated as the ratio of energy and capacity and reported in relation to the cell nominal voltage V_{nom}=3.7 V), life heat generation, life discharged chemical energy (defined as the sum of the life discharged electrical energy and the life heat generation), life average power, life average heat generation rate, and life average electro-chemical efficiency.

By analysing Figure 7, a Li-Ion cell temperature (T_{cell}) optimal range can be found to maximise the electrochemical efficiency, minimise the ageing rate, extend the operating life, and maximise the total energy discharged. In fact, when an isothermal condition in between 25°C and 35°C is imposed on the cell, the total life electrical energy discharged is higher than 150 Wh while the average power is kept higher than 2 W, the heat generation rate is lower than 0.4 W, the drop of the average operating voltage Vav is kept lower than 10% compared to the nominal value Vo, and the electrochemical efficiency is more than 85%. This range could be generally considered in line with an isoperibolic optimal temperature range of 25°C-40°C (the latter however not to be considered as truly universal leading to random isothermal conditions) as indicated by previous literature and reported in the introduction section. Importantly, within this isothermal temperature range, the experimental evidence would suggest 30°C as the best value to choose. When compared to the other values tested within this range, an isothermal temperature of 30°C leads to an appreciable gain in total operating life and consequent energy gain of around 330 Wh, i.e. twice the median value of the other temperatures tested in between 25°C and 35°C.

Table 10: Overall operating life discharge performance of Li-Ion cells at different isothermal conditions. In bold, the optimal temperature identified for this specific 300-mAh LCO-graphite Li-Ion pouch cell

T_{set}	Cap	E	V_{av}	Q	E_{ch}	P_{av}	$\dot{Q}_{av}$	η
0	1.76	5.32	3.02	2.01	7.33	1.81	0.683	72.61%
10	5.88	18.89	3.21	5.09	23.99	1.91	0.515	78.75%
20	20.10	66.89	3.32	11.57	78.46	1.99	0.345	85.26%
25	44.28	146.85	3.32	24.13	170.97	1.99	0.326	85.89%
27.5	41.60	140.32	3.37	22.67	162.98	2.02	0.326	86.09%
30	97.54	327.68	3.36	40.54	368.23	2.01	0.249	88.99%
35	46.14	157.40	3.41	18.25	175.65	2.05	0.237	89.61%
40	34.59	118.14	3.42	9.75	127.90	2.05	0.169	92.38%

Legend: T_{set}= Set Temperature [°C], Cap = discharged capacity [Ah] E = discharged energy [Wh], V_{av}=average voltage [V], Q = heat generation [Wh], E_{ch}=chemical energy [Wh] Pav=average power [W], $\dot{Q}_{av}$ = average heat generation rate [W], η=discharge efficiency

Therefore, it can be concluded that for this specific cell, i.e. for a 300-mAh LCO-graphite Li-Ion pouch cell, an actual optimal isothermal condition occurs in the range of 25°C-35°C and at approximately 30°C. However, it must be emphasised that these results are valid for this specific cell and cannot be easily extended to every Li-Ion cells, i.e. for all possible combinations of chemistries, capacities, and geometries. However, the comparison with the existing literature reported in the previous section, even if based on studies applying an isoperibolic boundary condition, would support this conclusion. In fact, most of these studies report a similar optimal

isoperibolic condition of 25°C which is reasonably close (mostly during the discharge phase) to an isothermal condition of 30°C.

4. Conclusions

Previous studies have largely focused on Li-Ion cells ageing under constant ambient or surrounding temperature (isoperibolic) thermal boundary conditions. This work employed the novel experimental approach proposed in Landini et al. [24] to analyse a Li-Ion cell ageing under isothermal conditions (i.e. uniform cell surface temperature). This is crucial as this is the likely operational scenario of any active cooling approach, as part of a Li-Ion cells Thermal Management System (TMS). Importantly, this is significantly different from an isoperibolic condition where the surface temperature and critically the rate of heat transfer from the cell would be significantly different from an active TMS. Also, the current approach would benefit the bespoke engineering design of TMS specifically for Li-Ion batteries at a cellular level.

The difference between applying an isoperibolic and an isothermal (i.e. stable uniform cell surface temperature) condition of 10°C, 25°C, and 35°C on a 300-mAh LCO-graphite Li-Ion pouch cell ageing has been presented. Interestingly, similar overall average ageing rates were found by comparing isoperibolic/isothermal conditions of 10°C/20°C, 25°C/30°C, and 35°C/35°C respectively. This was mainly attributed to the effect of the cell self-heating due to ohmic heat losses which forces the cell to operate at a median temperature higher than the surroundings. Importantly, this effect increases at lower temperatures, as the higher cell internal resistance leads to higher ohmic losses and higher temperature differences between surroundings and cell based on the same cooling capability of isoperibolic TMS. Crucially, this emphasises that uncontrolled cell thermal conditions lead to overall performance strongly dissimilar and dependent on the transient heat transfer coefficient of isoperibolic TMS.

Also, an ideal isothermal condition to reach a desired electrochemical efficiency and battery longevity, i.e. minimal ageing rate, has been identified for this specific cell's chemistry and geometry. The Li-Ion pouch cells were cycled continuously at different fixed cell temperatures in the range of 0°C-40°C under CR=1C and DR=2C until the EOL. Ageing was found to be highly sensitive to cell temperature. Both high and low temperatures lead to strong ageing and consequently short operating life. The temperature which minimised the ageing and guaranteed the longest operating life was 30°C (EOL=450 cycle, ageing rate of 0.034%/cycle). Temperatures

lower than 20°C and higher than 35°C led to an ageing rate of 10 and 4 times higher than at 30°C respectively. This is a rough estimate; however, it clearly highlights the significance and scale of the aging rate and its variance that can be experienced in application with these specific operating conditions. This is mainly attributed to the thermodynamic-driven irreversible cathode/electrolyte decomposition and SEI growth enhancement experienced at high temperatures versus the lithium loss due to Li plating at low temperatures.

By considering the cell overall life performance, a cell temperature optimal range was found to maximise the electrochemical efficiency, minimise the ageing rate, extend the operating life, and maximise the total energy discharged. When an isothermal condition in the range of 25°C and 35°C was imposed on the cell, the total life electrical energy discharged was higher than 150 Wh while the average power was kept higher than 2 W, the heat generation rate was lower than 0.4 W, the drop of the average operating voltage compared to the nominal value was kept lower than 10%, and the electrochemical efficiency was higher than 85%.

Therefore, it can be concluded that for this specific cell an actual optimal isothermal condition can be indicated to be in the range of 25°C- 35°C and around 30°C. It must be emphasised that these results are valid for this specific cell and cannot be easily extended to every kind of Li-Ion cells, i.e. for all possible combinations of chemistries, capacities, and geometries. However, the comparison with the literature would support this conclusion. In fact, most previous studies report an optimal isoperibolic condition of 25°C which is reasonably close to an isothermal condition of 30°C.

Future studies should focus on using the novel experimental approach based on an isothermal condition employed in this study to conduct systematic performance characterisation and ageing test campaign on Li-Ion cells of different capacities, sizes, cathode chemistries, and geometries. A robust dataset should be collected and evaluated to identify the optimal isothermal conditions of these cells, and investigate whether these conditions differ from the one identified in this study. In addition, a sound statistical analysis and modelling (e.g. multi-variable regression, neural network) should be proposed to create a universal model based on clearly comparable experimental data based on tests at isothermal and not isoperibolic conditions.

Acknowledgements

The authors would like to acknowledge Heriot-Watt University to fund this project through the James Watt Scholarship. The authors would like to express their gratitude to Dukosi Ltd. and Mr Josh Leworthy for providing the cooling chamber and giving support during the development of the test rig.

Data availability

Datasets related to this article can be found at https://doi.org/10.17632/f9mgvptpkn.1, an open-source online data repository hosted at Mendeley Data [25].

Reference

[1] S. Landini, J. Leworthy, T.S. O'Donovan, A Review of Phase Change Materials for the Thermal Management and Isothermalisation of Lithium-Ion Cells, J. Energy Storage. 25 (2019). https://doi.org/10.1016/j.est.2019.100887.

[2] S. Landini, R. Waser, A. Stamatiou, R. Ravotti, J. Worlitschek, T.S. O'Donovan, Passive cooling of Li-Ion cells with direct-metal-laser-sintered aluminium heat exchangers filled with phase change materials, Appl. Therm. Eng. 173 (2020) 115238. https://doi.org/10.1016/j.applthermaleng.2020.115238.

[3] C. Lin, S. Xu, Z. Li, B. Li, G. Chang, J. Liu, Thermal analysis of large-capacity LiFePO 4 power batteries for electric vehicles, J. Power Sources. 294 (2015) 633–642. https://doi.org/10.1016/j.jpowsour.2015.06.129.

[4] T. Waldmann, M. Wilka, M. Kasper, M. Fleischhammer, M. Wohlfahrt-Mehrens, Temperature dependent ageing mechanisms in Lithium-ion batteries e A Post-Mortem study, J. Power Sources. 262 (2014) 129–135. https://doi.org/10.1016/j.jpowsour.2014.03.112.

[5] A. Barré, B. Deguilhem, S. Grolleau, M. Gérard, F. Suard, D. Riu, A review on lithium-ion battery ageing mechanisms and estimations for automotive applications, J. Power Sources J. 241 (2013) 680–689. https://doi.org/10.1016/j.jpowsour.2013.05.040.

[6] M. Rosa Palací ab, Understanding ageing in Li-ion batteries: a chemical issue, Chem. Soc. Rev. 47 (2018) 4924. https://doi.org/10.1039/c7cs00889a.

[7] A. Barai, R. Tangirala, K. Uddin, J. Chevalier, Y. Guo, A. McGordon, P. Jennings, The effect of external compressive loads on the cycle lifetime of lithium-ion pouch cells, J. Energy Storage. 13 (2017) 211–219. https://doi.org/10.1016/j.est.2017.07.021.

[8] C.R. Birkl, M.R. Roberts, E. McTurk, P.G. Bruce, D.A. Howey, Degradation diagnostics for lithium ion cells, J. Power Sources. 341 (2017) 373–386. https://doi.org/10.1016/j.jpowsour.2016.12.011.

[9] P. Ramadass, B. Haran, R. White, B.N. Popov, Capacity fade of Sony 18650 cells cycled at elevated temperatures: Part I. Cycling performance, J. Power Sources. 112 (2002) 606–613. https://doi.org/10.1016/S0378-7753(02)00474-3.

[10] M. Dubarry, B.Y. Liaw, M.S. Chen, S.S. Chyan, K.C. Han, W.T. Sie, S.H. Wu, Identifying battery aging mechanisms in large format Li ion cells, J. Power Sources. 196 (2011) 3420–3425. https://doi.org/10.1016/j.jpowsour.2010.07.029.

[11] F. Leng, C.M. Tan, M. Pecht, Effect of Temperature on the Aging rate of Li Ion Battery Operating above Room Temperature, Sci. Rep. 5 (2015) 1–12. https://doi.org/10.1038/srep12967.

[12] Y. Wu, P. Keil, S.F. Schuster, A. Jossen, Impact of temperature and discharge rate on the aging of a LiCoO2/LiNi0.8Co0.15Al0.05O2 lithium-ion pouch cell, J. Electrochem. Soc. 164 (2017) A1438–A1445. https://doi.org/10.1149/2.0401707jes.

[13] H. Wang, S. Frisco, E. Gottlieb, R. Yuan, J.F. Whitacre, Capacity degradation in commercial Li-ion cells: The effects of charge protocol and temperature, J. Power Sources. 426 (2019) 67–73. https://doi.org/10.1016/j.jpowsour.2019.04.034.

[14] A. Friesen, X. Mönnighoff, M. Börner, J. Haetge, F.M. Schappacher, M. Winter, Influence of temperature on the aging behavior of 18650-type lithium ion cells: A comprehensive approach combining electrochemical characterization and post-mortem analysis, J. Power Sources. 342 (2017) 88–97. https://doi.org/10.1016/j.jpowsour.2016.12.040.

[15] M. Dubarry, C. Truchot, B.Y. Liaw, K. Gering, S. Sazhin, D. Jamison, C. Michelbacher, Evaluation of commercial lithium-ion cells based on composite positive electrode for plug-in hybrid electric vehicle applications. Part II. Degradation mechanism under 2 C cycle aging, J. Power Sources. 196 (2011) 10336–10343. https://doi.org/10.1016/j.jpowsour.2011.08.078.

[16] S. Liu, M. Winter, M. Lewerenz, J. Becker, D.U. Sauer, Z. Ma, J. Jiang, Analysis of cyclic aging performance of commercial Li 4 Ti 5 O 12-based batteries at room temperature, Energy. 173 (2019) 1041–1053. https://doi.org/10.1016/j.energy.2019.02.150.

[17] G. Ning, B. Haran, B.N. Popov, Capacity fade study of lithium-ion batteries cycled at high discharge rates, J. Power Sources. 117 (2003) 160–169. https://doi.org/10.1016/S0378-7753(03)00029-6.

[18] A. Schmidt, A. Smith, H. Ehrenberg, Power capability and cyclic aging of commercial, high power lithium ion battery cells with respect to different cell designs, J. Power Sources. 425 (2019) 27–38. https://doi.org/10.1016/j.jpowsour.2019.03.075.

[19] J. Yi, B. Koo, C.B. Shin, T. Han, S. Park, Modeling the effect of aging on the electrical and thermal behaviors of a lithium-ion battery during constant current charge and discharge cycling, Comput. Chem. Eng. 99 (2017) 31–39. https://doi.org/10.1016/j.compchemeng.2017.01.006.

[20] A. Shifa Mussa, A. Liivat, F. Marzano, M. Klett, B. Philippe, C. Tengstedt, G. Lindbergh, K. Edström, R.W. Lindström, P. Svens, Fast-charging effects on ageing for energy-optimized automotive LiNi 1/3 Mn 1/3 Co 1/3 O 2 /graphite prismatic lithium-ion cells, J. Power Sources. 422 (2019) 175–184. https://doi.org/10.1016/j.jpowsour.2019.02.095.

[21] B. Epding, B. Rumberg, H. Jahnke, I. Stradtmann, A. Kwade, Investigation of significant capacity recovery effects due to long rest periods during high current cyclic aging tests in automotive lithium ion cells and their influence on lifetime, J. Energy Storage. 22 (2019) 249–256. https://doi.org/10.1016/j.est.2019.02.015.

[22] M.A. Monem, K. Trad, N. Omar, O. Hegazy, B. Mantels, G. Mulder, P. Van Den Bossche, J. Van Mierlo, Lithium-ion batteries: Evaluation study of different charging methodologies based on aging process q, Appl. Energy. 152 (2015) 143–155. https://doi.org/10.1016/j.apenergy.2015.02.064.

[23] A. Shifa Mussa, M. Klett, M. Behm, G. Lindbergh, R.W. Lindström, Fast-charging to a partial state of charge in lithium-ion batteries: A comparative ageing study, J. Energy Storage. 13 (2017) 325–333. https://doi.org/10.1016/j.est.2017.07.004.

[24] S. Landini, T.S. O'Donovan, Novel experimental approach for the characterisation of Lithium-Ion cells performance in isothermal conditions, Energy. 214 (2020) 118965.

https://doi.org/10.1016/j.energy.2020.118965.

[25] S. Landini, T.S. O'Donovan, Experimental Investigation of Lithium-Ion Cells Ageing under Isothermal Conditions for Optimal Lifetime Performance: Datasets and Supplementary Materials, Mendeley Data, V1, (2021). https://doi.org/10.17632/f9mgvptpkn.1.

[26] R. Srinivasan, A. Carson Baisden, B.G. Carkhuff, M.H. Butler, The five modes of heat generation in a Li-ion cell under discharge, J. Power Sources. 262 (2014) 93–103. https://doi.org/10.1016/j.jpowsour.2014.03.062.